4. Zaikin, A. N. & Zhabotisnky, A. M. *Nature* **225,** 535–537 (1970).
5. Winfree, A. T. *Science* **175,** 634–636 (1972).
6. Agladze, K. I., Krinsky, V. I. & Pertsov, A. M. *Nature* **308,** 834–835 (1984).
7. Maselko, J. & Showalter, K. *Physica* D**49,** 21–32 (1991).
8. Steinbock, O., Zykov, V. & Müller, S. C. *Nature* **366,** 322–324 (1993).
9. Markus, M., Kloss, G. & Kusch, I. *Nature* **371,** 402–404 (1994).
10. Nagy-Ungvarai, Zs. & Müller, S. C. *Int. J. Bifurc. Chaos* **4,** 1257–1264 (1994).
11. Noszticzius, Z., Horsthemke, W., McCormick, W. D., Swinney, H. L. & Tam, W. Y. *Nature* **329,** 619–620 (1987).
12. Skinner, G. & Swinney, H. L. *Physica* D**48,** 1–16 (1991).
13. Dulos, E., Boissonade, J. & De Kepper, P. *Physica* A**188,** 120–131 (1992).
14. Oyang, Q. & Swinney, H. L. *Nature* **352,** 610–612 (1991).
15. Ouyang, Q. & Swinney, H. L. *Chaos* **1,** 411–420 (1991).
16. Kramer, L., Hynne, F., Sørenson, P. G. & Walgraef, D. *Chaos* **4,** 443–452 (1994).
17. Sørenson, P. G. & Hynne, F. *J. phys. Chem.* **93,** 5467–5474 (1989).
18. Landau, L. D. & Lifshitz, E. M. *Fluid Mechanics* (Pergamon, Oxford, 1959).
19. Huerre, P. in *Propagation Far from Equilibrium* (ed. Weisfred, J. E., Brand, H. R., Manneville, P., Albinet, G. & Boccara, N.) 340–353 (Springer, Berlin, 1988).
20. Manneville, P. in *Structures Dissipatives, Chaos et Turbulence* 349–352 (Aléa-Saclay, 1991).
21. Fauve, S. in *Instabilities and Nonequilibrium Structures* (eds Tirapegui, E. & Villaroel, D.) 63–88 (Reidel, Dordrecht, 1987).
22. Janiaud, B., Pumir, A., Bensimon, D., Croquette, V., Richter, H. & Kramer, L. *Physica* D**55,** 269–286 (1992).

ACKNOWLEDGEMENTS. We thank Ch. Dupont for doing the numerical simulation, P. Coullet for suggesting the theoretical interpretation, and A. Belmonte, L. Gil, V. Krinsky, J. Lega and V. Voignier for discussions. Q.O. is on leave from the Physics Department, University of Texas at Austin.

Pathways of water between the Pacific and Indian oceans in the Indonesian seas

Arnold L. Gordon* & Rana A. Fine†

* Lamont-Doherty Earth Observatory, Columbia University, Palisades, New York 10964-8000, USA
† Rosenstiel School of Marine and Atmospheric Sciences, University of Miami, Miami, Florida 33149, USA

The physical structure of the Pacific and Indian oceans is substantially affected by the inter-ocean transport of excess fresh water from the North Pacific Ocean through the Indonesian seas[1,2]. The efficiency of this transport is an important regulator of the meridional overturning of these oceans[1,2], and hence perhaps of the global thermohaline circulation[3]; in addition, the seepage of warm water out of the Pacific affects the volume of the western Pacific warm pool, and thus may influence El Niño events[24]. But the sources, pathways and physical properties of the Indonesian throughflow are not well enough characterized to allow its influence on ocean circulation and the climate system to be quantified. Here we report salinity, temperature and chemical-tracer data from the Indonesian seas which show that the throughflow is dominated by two components: one of low-salinity, well ventilated North Pacific water through the upper thermocline of the Makassar Strait, and the other of more saline South Pacific water through the lower thermocline of the eastern Indonesian seas. Seasonal (monosonal) variations in the ratio of these components, perhaps modulated by El Niño conditions, imply the existence of potentially important variable feedbacks to the ocean circulation and climate system.

Recent observational studies offer a wide range of estimates for the Indonesian throughflow (Fig. 1), from 7 to 18.6 $\times 10^6$ m^3 s^{-1} (refs 4–6) including 1.7 $\times 10^6$ m^3 s^{-1} within the Lombok Strait[7]. Density-driven overflow via the 1,940-m-deep Lifamatola Passage into the depths of the Banda Sea[8] contributes a minor amount to the total throughflow, approximately 10^6 m^3 s^{-1} (1 sverdrup). Water mass indicators suggest[3,9–12] that the throughflow occurs mainly within the thermocline and is drawn from the North Pacific, although this too remains a point of debate[13,14].

The Arlindo programme[13] measured the thermohaline and chlorofluorocarbon (CFC-11 and CFC-12) stratification within

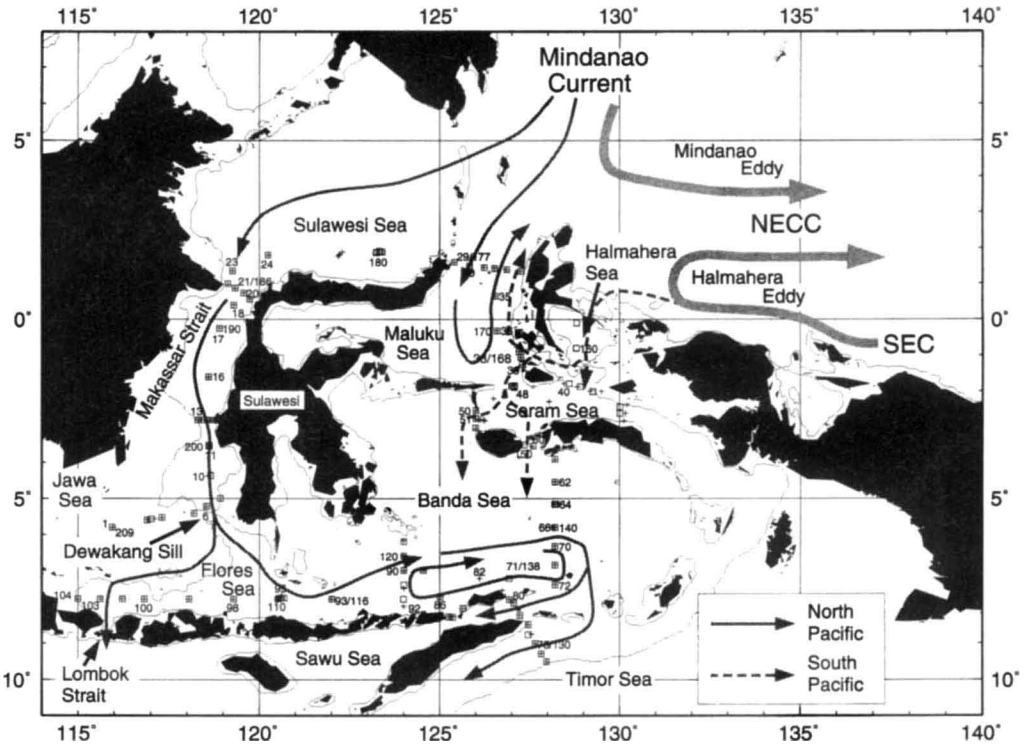

FIG. 1 Map of the oceanographic stations where measurements were obtained by the Arlindo programme, place names referred to in the text, and a schematic representation of the water spreading patterns in the Indonesian seas. The Arlindo oceanographic observations within the Indonesian seas consist of measurement of the temperature, salinity and oxygen stratification (CTD stations) and chlorofluorocarbon (CFC-11 and CFC-12) determinations. The data were obtained from the Indonesian R/*V Baruna Jaya I* during the southeast monsoon of 1993 (6 August to 12 September, stations 1–103, + symbols) and northwest monsoon of 1994 (25 January to 3 March, stations 104 to 209, □ symbols, many co-located with 1993 stations). The positions of stations used in Figs 2 and 3 are indicated. A schematic of the thermocline circulation pattern, based on water mass analysis, is indicated by the arrows denoting spreading pathways of North and South Pacific thermocline water masses. NECC is the North Equatorial Countercurrent, SEC is the South Equatorial Current. The Makassar Strait, carrying North Pacific water, is the dominant throughflow pathway. There appears to be a minor contribution of North Pacific water along pathways east of Sulawesi. The South Pacific supplies relatively saline lower-thermocline water and all of the deeper water via the pathways east of Sulawesi. The lack of evidence for advective spreading indicates that there is not much transport associated with the South Pacific thermocline water.

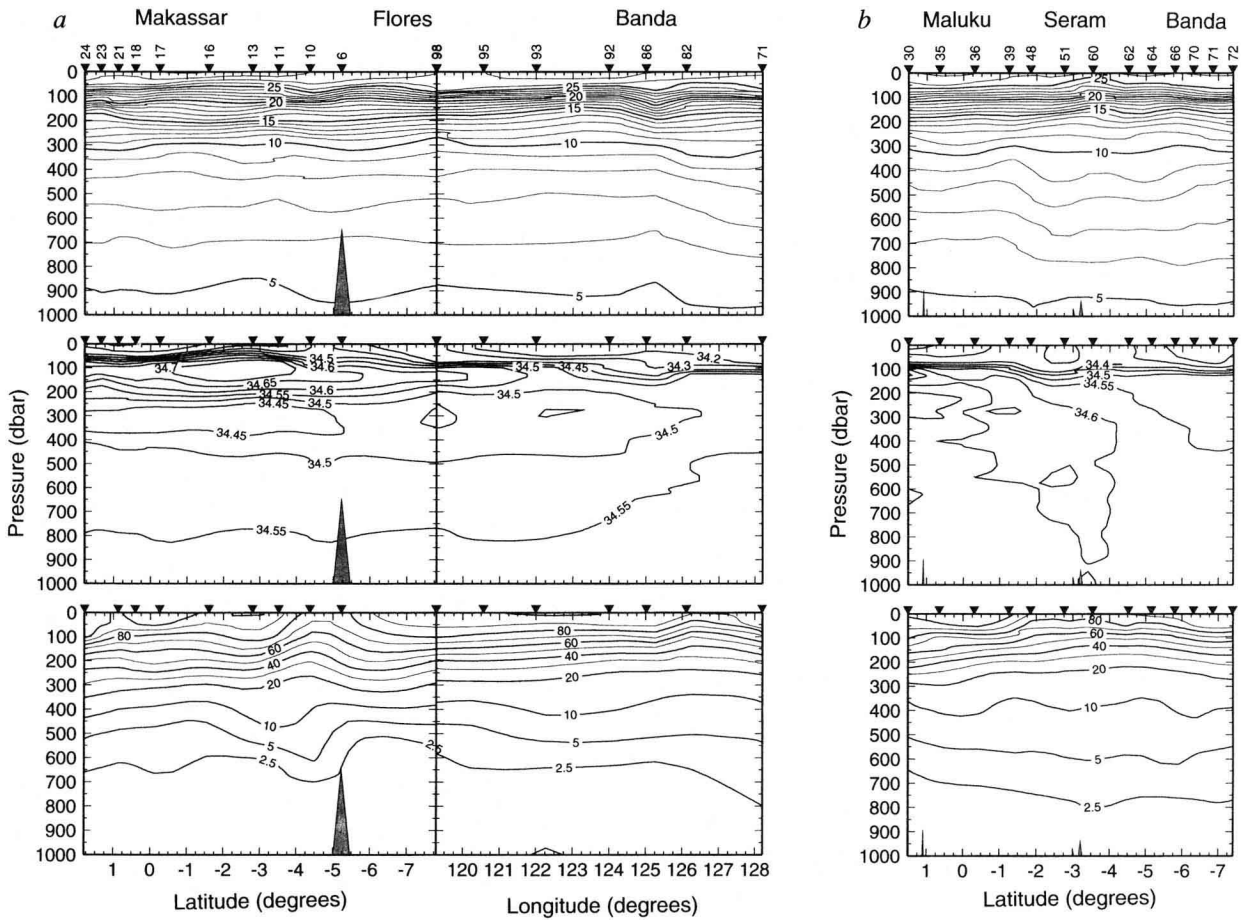

FIG. 2 Sections of (top to bottom in *a* and *b*) potential temperature (°C), salinity (p.p.t.) and percentage saturation (relative to the present atmosphere) of CFC-11 during the 1993 southeast Monsoon. Filled triangles at the top of each panel represent the station positions. The triangle on the bottoms of each panel at station 6 marks the shallowing at the Dewakang sill (Fig. 1). *a*, Sections along the Makassar Strait, Flores Sea into the southern Banda Sea. The stratification along the Makassar Strait and Flores Sea reveals the primary thermocline throughflow water masses of the region: the salinity maximum (*S*-max) near 125 dbar (1 dbar pressure ≈1 m) and mode water (marked by a slight reduction in the temperature gradient near 17 °C, 175 dbar at the same stations displaying a strong *S*-max) are derived from the North Pacific subtropical region; the salinity minimum (*S*-min) near 300 dbar is derived from the North Pacific Intermediate Water. *b*, Sections across the Maluku Sea, Seram Sea and Banda Sea. The northern Maluku Sea thermocline has similar properties to that of the Makassar Strait, but in the southern Maluku and in the Seram Sea the North Pacific *S*-max and *S*-min cores are absent, replaced by a lower-thermocline salinity maximum derived from the South Pacific thermocline. The southern Banda Sea thermocline more closely resembles that of the Flores, indicating it as its source. The corresponding NWM section (not shown) reveals slightly more concentrated South Pacific *S*-max in the Seram Sea.

the Indonesian seas during the 1993 southeast monsoon (SEM) and 1994 northwest monsoon (NWM) (Fig. 1). North Pacific salinity and CFC stratification features penetrate into the Banda Sea within the westernmost deep pathway from the Makassar Strait through the Flores Sea (Fig. 2*a*). Within the eastern throughflow route of Maluku to Seram to the Banda Sea (Fig. 2*b*), the North Pacific stratification features are discontinuous. Although the salinity maximum (*S*-max) and minimum (*S*-min) layers are persistent along the Makassar route, they do attenuate with distance from their entry at the Sulawesi Sea, as vertical mixing and dilution with local freshwater input diminishes the salinity stratification[10]. The *S*-max decrease is not uniform, as local pockets of elevated *S*-max are observed in the Makassar Strait in both monsoons, possibly denoting an uneven injection of North Pacific water.

In the southern Maluku and Seram seas (Fig. 2*b*), the North Pacific middle and lower thermocline is replaced by water too salty to be derived from the North Pacific. This water is South Pacific thermocline water which enters the Seram Sea through the Halmahera Sea, drawn from the New Guinea Coastal Undercurrent[11]. Similarity of the Maluku and Seram Sea low-salinity water within the upper 100 dbar to that of the Banda Sea (with dissimilarity to Sulawesi Sea surface water) suggests that the surface flow is towards the north, consistent with surface current charts[15].

CFC-11 can be used to identify the water masses in the Indonesian seas that are involved in decadal timescale climate processes. Based on the CFC-11 partial pressures[16], waters in the upper 200 dbar have been in contact with the atmosphere in the past 5 to (at most) 18 years in Makassar as compared with 13 to (at most) 22 years in Banda. The strongest age gradient occurs above 300 dbar (Fig. 2), similar to the Mindanao Current[11]. The recently ventilated (with respect to atmospheric gases) waters from the Mindanao Current observed in the Makassar above 300 dbar, particularly during the SEM, are mixed down and redistributed. In addition, during the NWM there is an input of South Pacific lower thermocline and intermediate water that is more highly saturated with CFC-11. As a consequence these layers in the Banda Sea waters are more highly saturated in CFC-11 than those of the Makassar or Maluku (Fig. 3), and they ultimately spread into and ventilate the Indian Ocean.

In the northern entrance to the Makassar Strait and the Maluku

Sea, the relationships between potential temperature T and salinity (T/S) or percentage saturation with CFC-11 (T/%CFC) (Fig. 3*a*) are very similar—though with diminished S-max, S-min and CFC-11 cores—to that of the Mindanao Current[13]. At the S-min core, the Makassar T/S relationship bears a closer resemblance to the inshore edge of the Mindanao Current, whereas the Maluku T/S is similar to the off-shore Mindanao Current. We suspect that the fine structure in the Maluku S-max layer is derived from the saltier South Pacific thermocline water observed in the southern Maluku Sea and the Seram Sea; this is particularly evident in the northeastern edge of the Maluku, suggesting an anti-clockwise circulation pattern within the Maluku thermocline (Fig. 1). The South Pacific thermocline water is seen in more concentrated form in the Seram Sea, and can only be derived from the Halmahera Sea. We note that the continuity of the North Pacific thermocline water between the Maluku Sea and Banda Sea is severed in the Seram Sea by the South Pacific thermocline water. However, deeper South Pacific water (below the Halmahera Sea sill depth of 500 dbar, and which therefore must be drawn from the Mindanao Current) is continuous from the Maluku to the Banda Sea, spilling into the deep Banda Sea over the Lifamatola sill[8].

In the Makassar, the S-max and %CFC are decidedly weaker in the NWM. We suggest that this reflects a relaxation of the throughflow during the NWM, with continued mixing in the Makassar Strait acting to attenuate the resident S-max and CFCs. The prevalence of 50-dbar-thick homogeneous layers or 'steps' in the Makassar thermocline indicate the presence of strong mixing[17]. Relaxation of the throughflow in the NWM is

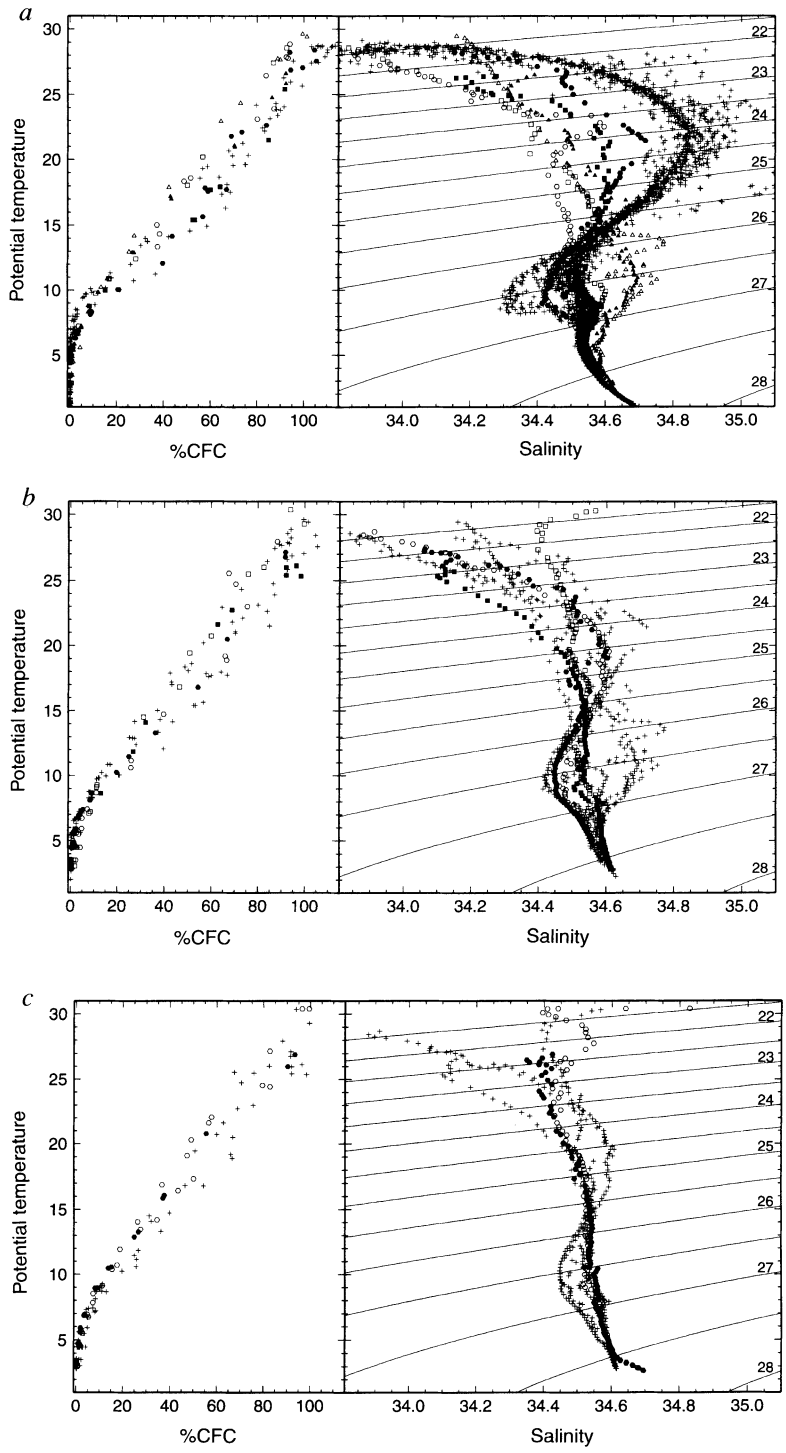

FIG. 3 Scatter plots of potential temperature/salinity (T/S) and potential-temperature/percentage saturation CFC-11 (T/%CFC) relationship for selected stations within the Indonesian Seas. The curved lines within the T/S plot marked 22–28 are lines of equal density (isopycnals) in σ_0 nomenclature. Due to the sparser resolution for CFCs, multiple and nearby stations are used to fill out the %CFC profile. Solid symbols represent the southeast Monsoon (SEM); open symbols represent the northwest Monsoon (NWM). *a*, The northern Indonesian seas. Circles show Makassar Strait stations, the T/S data are derived from stations 21 and 186; the %CFC data are derived from the stations 17, 18, 21, 186, 189 and 190 for the NWM. Boxes show the Maluku Sea, the T/S data are derived from stations 29 and 177; the %CFC data are derived from the stations 30 and 176. Triangles show the Seram Sea, the T/S data are derived from stations 38 and 168; the %CFC data are derived from the stations 38, 39, 167 and 169. *R/V Moana Wave* stations 3–36 (stations from May 1989 spanning the Mindanao Current west of 140° E between 8° and 9° N; ref 23) are shown as a +, as reference for the Arlindo T/S and T/%CFC scatter. The *Moana Wave* stations west of 127.67° E (within 115 km of the continental shelf) are responsible for the low-salinity feature in the 8–13 °C temperature interval, making a rather abrupt transition from more saline water to the east. It is this water that can be traced into the Makassar Strait. *b*, The southern Indonesian seas. Circles show the Flores stations, the T/S data are derived from stations 93 and 116; the %CFC data are derived from the stations 96, 97, 113 and 114. Boxes show the Banda Sea, the T/S data are derived from stations 71 and 138; the %CFC data are derived from stations 70, 71, 138 and 139. The northern data (from Fig. 3a) are shown as a + for reference. c, Timor Sea. Circles shows the T/S and T/%CFC relation for the Timor Sea, the T/S data are derived from stations 75 and 130; the %CFC data are derived from the stations 74, 75, 128, 129, 130. The Flores and Banda sea (Fig. 3*b*) are shown as a + for reference.

consistent with the model results[18]. The Flores Sea *S*-max and %CFC are stronger in the NWM, suggesting a monsoon phase lag of the *S*-max core layer between the Makassar and Flores. Considering the path length and width of Makassar Strait, a mean throughflow speed for the upper 300 m of 7 cm s^{-1} (corresponding to a transport of 5 sverdrup) would account for the phase lag.

In the Flores and Banda seas (Fig. 3*b*), the properties are similar to that of Makassar Strait, though in the Banda Sea the lower thermocline has somewhat elevated salinity indicating encroachment of South Pacific water via the Seram Sea[19] and the accumulated effects of mixing as discussed above. The Flores and Banda *T*/*S* curves match below the 5 °C isotherm. As this water is deeper than the Dewakang sill of southern Makassar Strait, it is totally derived from the Seram Sea. Above the 4 °C isotherm, the Timor Sea properties match that of the Banda Sea (Fig. 3*c*), indicating that the Banda Sea is the source of Timor Sea stratification. Below 4 °C the Timor water column is blocked from the southern Banda Sea by a 1,400-m sill[4]; the deeper more saline water within the Timor Sea is derived from the Indian Ocean[5].

The Arlindo data set unequivocally shows that the throughflow source and path is that of North Pacific thermocline water flowing from the Makassar Strait into the Flores and Banda Seas before curling southwards into the Timor Sea and Indian Ocean. East of Sulawesi there is little evidence of North Pacific throughflow within the upper thermocline, but the presence of relatively salty, lower-thermocline water suggests a direct contribution from South Pacific Ocean via the Halmahera Sea. Below the thermocline and Halmahera sill depth, the source of the Indonesian water is drawn from South Pacific but by a more indirect route involving transfer of water from the Mindanao Current to the Maluku Sea.

The inter-ocean throughflow pathway appears to follow the westernmost course of least impedance. To model realistically the throughflow pathway and source, it is becoming increasingly clear that it is critical to model very accurately the vigorous vertical mixing and geometry of the Indonesian region. This is needed not only to derive a realistic transport pattern, but also to reflect the correct ratio of North to South Pacific contribution to the throughflow at various depths[20]. Results of a recent modelling study[21], although fairly realistic, force most of the Makassar throughflow through the Lombok Strait rather than into the Flores Sea and fail to show saline South Pacific lower-thermocline water infiltrating the Seram Sea, instead showing surface South Pacific water entering the Seram. A model that fails to faithfully reproduce the source water ratio would be forced to find unrealistic ways to balance the hydrological cycle of the Pacific and Indian oceans[22].

The Arlindo programme occurred during a prolonged El Niño/Southern Oscillation (ENSO) event, though there was some relaxation of the southern oscillation index in January 1994, before plunging again into an El Niño condition in early 1994. The seasonal cycle of the source water, as revealed by the Arlindo data, opens the possibility of that the ratio of the North to South Pacific throughflow changes in response to the phase of ENSO, which may in turn provide feedback to ENSO by influencing the extent of the warm pool. The El Niño phase with diminished warm-pool presence in the western Pacific may be an analogue to the northern-winter, NWM condition, when the warm pool shifts southwards[24], diminishing its presence at the throughflow entrances. The La Niña phase would then correspond to the northern summer, SEM condition, when the warm-pool presence at the entrances is strengthened[24]. □

Received 26 May; accepted 28 November 1995.

1. Piola, A. & Gordon, A. *J. phys. Oceanogr.* **16,** 2184–2190 (1986).
2. MacDonald, A. *J. geophys. Res.* **98,** 6851–6868 (1993).
3. Gordon, A. *J. geophys. Res.* **91,** 5037–5047 (1986).
4. Cresswell, G., Frische, A., Peterson, J. & Quadfasel, D. *J. geophys. Res.* **98,** 14379–14390 (1993).
5. Fieux, M. *et al. Deep-Sea Res. Pt I* **41,** 1091–1130 (1994).
6. Meyers, G., Bailey, R. & Worby, A. *Deep-Sea Res. Pt I* **42,** 1163–1174 (1995).
7. Murray, S. & Arief, D. *Nature* **333,** 444–447 (1988).
8. Van Aken, H. M., Punjanan, J. & Saimima, S. *Neth. J. Sea Res* **22,** 315–339 (1988).
9. Fine, R. *Nature* **315,** 478–480 (1985).
10. Ffield, A. & Gordon, A. *J. phys. Oceanogr.* **22,** 184–195 (1992).
11. Fine, R., Lukas, R., Bingham, F., Warner, M. & Gammon, R. *J. geophys. Res.* **99,** 25063–25080 (1994).
12. Wyrtki, K. *J. geophys. Res.* **92** 12941–12946 (1987).
13. Gordon, A. *J. Phys. Oceanogr.* **25,** 1560–1567 (1995).
14. Godfrey, S., Hirst, A. & Wilkin, J. *J. Phys. Oceanogr.* **23,** 1087–1098 (1993).
15. Wyrtki, K. NAGA Rep. 2 (Scripps Inst. Oceanogr, La Jolla, 1961).
16. Doney, S. C. & Bullister, J. L. *Deep-Sea Res. Pt I* **39,** 1857–1883 (1992).
17. Ffield, A. thesis, Columbia Univ. (1994).
18. Kindle, J. C., Hurlburt, H. E. & Metzger, J. *Proc. Western Pacific Int. Mtg & Workshop on TOGA COARE* (eds Picaut, J., Lukas, R. & Delcroix, T.) 355–365 (Univ. Hawaii, Honolulu, 1989).
19. Gordon, A., Ffield, A. & Ilahude, A. G. *J. geophys. Res.* **99,** 18235–18242 (1994).
20. Nof, D. *J. phys. Oceanogr.* **25,** 1369–1383 (1995).
21. Miyama, T., Awaji, T., Akitomo, K. & Imasato, N. *J. Geophys. Res.* **100,** 20517–20541 (1995).
22. Piola, A. & Gordon, A. *J. phys. Oceanogr.* **14,** 747–753 (1984).
23. Johnson, G. & Toole, J. *Deep-Sea Res.* **40,** 371–394 1993).
24. Wyrtki, K. in *Proc. Western Pacific Int. Mtg & Workshop on TOGA COARE* (eds Picaut, J., Lukas, R. & Delcroix, T.) 99–109 (Univ. Hawaii, Honolulu, 1989).

ACKNOWLEDGEMENTS. We thank M. T. Zen, I. Soesilo, A. Soegiarto, K. Romimohtarto and A. Nontji for their help, and A. G. Ilahude for assistance in organizing the Arlindo cruises. We also thank the captain and crew of the R/V *Baruna Jaya I*, and the US and Indonesian scientific team, for their fine support, particularly B. Huber, P. Mele, A. Ffield, K. Sullivan, K. Maillet, J. Belinne and Mushwerry.

Thermal structure of a fossil mantle diapir inferred from the distribution of mafic cumulates

Georges Ceuleneer, Marc Monnereau & Isma Amri

Centre National de la Recherche Scientifique, UPR 234, Observatoire Midi-Pyrénées, 14, avenue Edouard Belin, 31400 Toulouse, France

Mafic lithologies constitute a minor but ubiquitous component of the mantle section of ophiolites; they are currently viewed as cumulates left by basaltic melts travelling from the melting region to the surface. These features may be used to constrain the mechanisms of melt migration in the mantle, provided their geophysical context of emplacement can be established in some detail. Here we report on the nature and distribution of mafic cumulates in the harzburgites of the Oman ophiolite, within and around a mantle diapir frozen beneath a spreading axis[1–6]. We show that their composition, texture and field characteristics are systematically related and display a concentric zoning centred on the diapir. We propose that this zoning reflects the thermal structure of the diapir and of the associated melt plumbing system. Assuming a parental liquid with the composition of mid-ocean-ridge basalt[7–9], the cumulate compositions show that the melt temperature exceeded 1,230 °C in the innermost part of the diapir and decreased progressively down to <1,100 °C in the surrounding lithospheric mantle. The transition between channelled porous flow and dyking is observed in an outer shell of the diapir, where the melt crystallized along the plagioclase–olivine cotectic (temperature ranging from 1,180 to 1,210 °C).

Mafic cumulates scattered within outcrops of mantle peridotites display a wide spectrum of field characteristics, indicative of the diversity of small-scale processes involved in melt migration: convincing evidence has been reported for contrasting mechanisms such as fracture, dissolution and compaction[4,5,10–15]. There are, however, important differences among authors concerning the attribution of a mechanism (or combination of mechanisms) to a particular geophysical context. Among others, the problem of the transition between intergranular porous flow and dyking—the 'brittle–ductile' transition for melt transport in the mantle—is still eagerly debated. Do fractures develop in the partially molten mantle or are they restricted to the cooler litho-